



Overall effective elastic properties of composites by computational homogenization

Wanderson F. dos Santos¹, Ayrton R. Ferreira¹, Sergio P. B. Proença¹

¹*São Carlos School of Engineering, University of São Paulo
Av. Trab. São Carlense, 400, Zip-Code: 13566-590, São Carlos, São Paulo, Brazil
wanderson_santos@usp.br, ayrton.ferreira@usp.br, persival@sc.usp.br*

Abstract. In composite materials the combination of different constituents promotes heterogeneity and specific properties. Therefore, the constitutive behavior of a composite can be complex. In this context, the present work explores a computational homogenization procedure to predict the overall or macroscopic effective elastic properties accounting for characteristics of the constituents at microscale. The microstructure of the material is modeled using the concept of Representative Volume Element (RVE). Both uniform strain or periodic boundary condition are applied on the RVE to compare the results. The effective elastic properties are then obtained from homogenization of the microscopic fields computed with three-dimensional numerical simulations by finite elements. The macroscopic constitutive properties obtained numerically are then compared to available results. The results show a strong influence of the boundary condition on the effective elastic properties. On the other hand, the inclusion morphology has no significant influence on the results. Furthermore, the procedure hereby described is an effective tool to the more realistic modeling of the macroscopic constitutive behavior of composites materials.

Keywords: Composite materials, Computational homogenization, Overall effective elastic properties, Uniform strain boundary condition, Periodic boundary condition.

1 Introduction

Composite materials are widely used in many industrial segments, such as Civil Engineering, Aerospace Engineering and Mechanical Engineering. An advantage is the combination of particular material properties to create an improved material with improved specific properties. However, the constitutive behavior of a composite material can be highly complex due to the heterogeneity observed in the lower scales. Therefore, further studies are justified to model with more accuracy the constitutive behavior of this class of materials.

One of the fields of interest in the study of composite materials is the prediction of the overall effective elastic properties. Some precursor works in this sense were Voigt [1] (providing an upper bound) and Reuss [2] (providing a lower bound). The model of Voigt [1] assumes that the deformation field is uniform in the composite. On the other hand, the model of Reuss [2] assumes that the stress field is uniform in the composite. Despite these analytical models are based on simplified assumptions, they provide rigorous reference limits in the study of effective elastic properties. The analytical expressions derived from variational principles by Hashin and Shtrikman [3] giving more precise bounds are also well-known. Another classic work worth to be mentioned is Hill [4], where important concepts about representative volume and relations between averages are discussed.

In the last decades, many works have been developed considering approaches based on computational homogenization using finite elements to study the effective elastic properties of composite materials. Sun and Vaidya [5] computed the effective elastic properties of periodic composites considering the concept of Representative Volume Element (RVE). Michel et al. [6] studied the effective properties of several specific problems of composites with periodic microstructure composed of linear or non-linear constituents. Xia et al. [7] presented an explicit unified form of boundary conditions for a periodic RVE. Kari et al. [8] assessed the effective material properties of composites reinforced by randomly distributed spherical particles. Medeiros et al. [9] evaluated the effective properties for smart composite materials with piezoelectric fibers embedded in a non-piezoelectric matrix (epoxy resin). More recently, Omairey et al. [10] developed an ABAQUS[®] plugin to estimate the homogenized elastic

properties for a periodic RVE of a composite material.

In this context, the present work explores a computational homogenization procedure to obtain the overall effective elastic properties of composite materials. The homogenization procedure is implemented in the ANSYS[®] Mechanical, Release 18.0. The study assesses the influence of the inclusion morphology on the effective elastic properties of composites considering: (1) Cubic cell with a unidirectional inclusion of circular cross section; (2) Cubic cell with a unidirectional inclusion of square cross section. The results are compared considering two boundary conditions: (i) Uniform strain boundary condition; (ii) Periodic boundary condition.

2 Preliminary concepts: homogenization and effective properties

The average-based homogenization theory is interesting for the study of the overall homogenized constitutive response of composite materials. In this case, the macroscopic stress and strain fields associated with the macroscale of the continuum (Σ and E) are obtained by the volume averaging of the respective microscopic fields or RVE fields (σ and ε) [11]:

$$\Sigma = \frac{1}{V} \int_V \sigma dV = \langle \sigma \rangle; \quad E = \frac{1}{V} \int_V \varepsilon dV = \langle \varepsilon \rangle \quad (1)$$

where $\langle \cdot \rangle$ indicates volume averaging; V represents the total initial volume of the RVE (for small strains).

The Hill-Mandel principle (see Bishop and Hill [11] and Mandel [12]) associates the macroscale and microscale domains. According to this principle, an equivalence of energy is assumed on both scales:

$$\Sigma : E = \frac{1}{V} \int_V \sigma : \varepsilon dV = \langle \sigma : \varepsilon \rangle \quad (2)$$

The stress and strain tensors in the macroscale can be correlated by an effective elastic stiffness tensor (\mathbb{C}) or an effective elastic flexibility tensor ($\mathbb{D} = \mathbb{C}^{-1}$), both being a fourth-order tensor presenting major and minor symmetries:

$$\Sigma = \mathbb{C} : E; \quad E = \mathbb{D} : \Sigma \quad (3)$$

Since Σ and E are averages of σ and ε over the volume, a Boundary Value Problem (BVP) must be solved to evaluate the microscopic fields of the RVE. Two classes of boundary conditions often appointed in the literature are: (i) Uniform strain boundary condition (USBC); and (ii) Periodic boundary condition (PBC). The USBC assumes that the displacements imposed on the outer contour of the RVE are compatible with a macroscopic homogeneous strain state (E^*):

$$u = E^* \cdot x \quad \forall \quad x \in \partial V \quad (4)$$

where $E = \langle \varepsilon \rangle = E^*$ and x is the position vector. An illustrative scheme of the USBC is shown in Figure 1(a).

In turn, the PBC comprises a parcel associated with the macroscopic homogeneous strain (E^*) and a parcel called periodic fluctuation (\tilde{u}):

$$u = E^* \cdot x + \tilde{u} \quad \forall \quad x \in \partial V \quad (5)$$

where $E = \langle \varepsilon \rangle = E^*$.

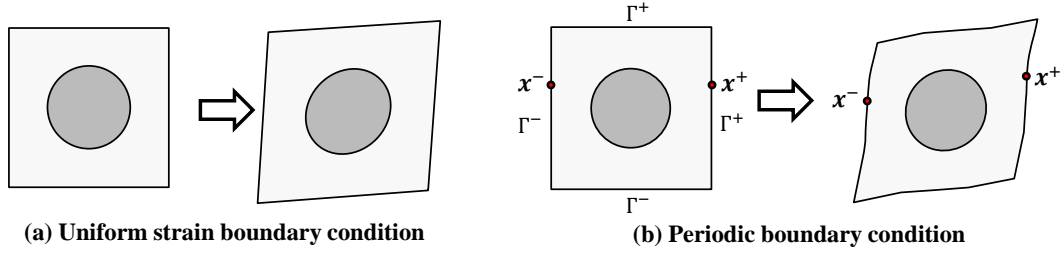


Figure 1. Illustration of two classes of boundary conditions.

However, the \tilde{u} variable is not known initially in the BVP for the PBC. An alternative for the implementation of PBC is to correlate the displacement of the outer contour nodes by restrictions in the BVP (e.g. by means of Lagrange multipliers or penalty function method). In this case, the outer contour of the RVE can be divided into a positive part (Γ^+) and a negative part (Γ^-). Thus, each point x^+ on Γ^+ has a corresponding point x^- on Γ^- . An illustrative scheme of the PBC is shown in Figure 1(b). For example, considering the points x^+ and x^- , we have the following restriction in the BVP for PBC:

$$\mathbf{u}^+ - \mathbf{u}^- = \mathbf{E} \cdot (\mathbf{x}^+ - \mathbf{x}^-) \quad (6)$$

where $\tilde{\mathbf{u}}^+ - \tilde{\mathbf{u}}^- = 0$.

The same conceptual approach can be extended to a three-dimensional (3D) RVE for the implementation of the periodic condition. An alternative is to divide the outer contour of the RVE considering groups of S_{face} (faces), S_{edge} (edges) and S_{corner} (corners) (see Figure 2).

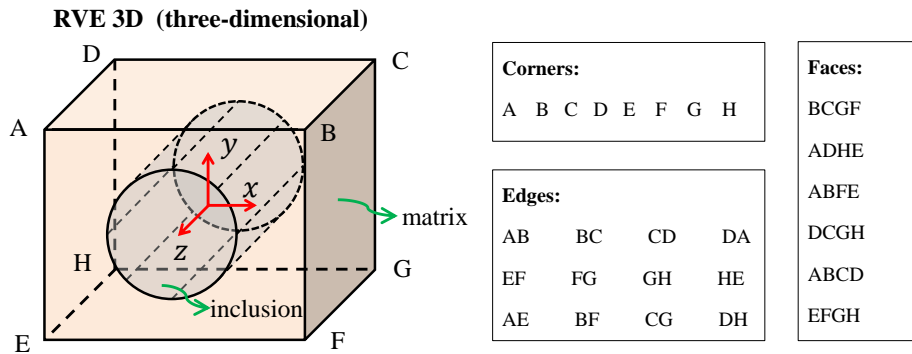


Figure 2. Groups S_{face} (faces), S_{edge} (edges) and S_{corner} (corners) on the outer contour of the RVE.

After creating the RVE finite element mesh, the nodes for each group (S_{face} , S_{edge} and S_{corner}) can be correlated by eq. (6) considering the pairs (see more details in Santos [13]):

$$S_{\text{face}} = \{ (BCGF, ADHE), (ABCD, EFGH), (ABFE, DCGH) \}$$

$$S_{\text{edge}} = \{ (BF, CG), (BF, AE), (AE, DH), (AB, CD), (AB, EF), (EF, GH), (BC, AD), (BC, FG), (FG, EH), (AD, EH), (CD, GH), (CG, DH) \}$$

$$S_{\text{corner}} = \{ (B, C), (C, G), (G, F), (A, G), (D, H), (H, E), (E, F), (B, A), (A, E), (B, F), (C, D), (G, H) \}$$

2.1 Effective elastic properties of composites by computational homogenization

In this section, the computational homogenization procedure to study the effective elastic properties of composites is presented. The study is carried out for two periodic RVE morphologies (see Fig. 3): (i) RVE1 - Cubic cell with a unidirectional inclusion of circular cross section; (ii) RVE2 - Cubic cell with a unidirectional inclusion

of square cross section. The constitutive behavior for the matrix and for inclusion is linear elastic. The modulus of elasticity (Y), the Poisson's ratio (ν) and the volume fraction (f) of each constituent are adopted following Xia et al. [7], Sun and Vaidya [5]. The aluminum matrix has $Y_m = 68.3$ GPa, $\nu_m = 0.3$ and $f_m = 0.53$. The boron inclusion has $Y_i = 379.3$ GPa, $\nu_i = 0.1$ and $f_i = 0.47$.

The homogenized constitutive behavior of each RVE is obtained for the USBC and PBC. Both kinematic boundary conditions are written as a function of a macroscopic strain imposed on the external contour of the RVE (\mathbf{E}^*). In these cases, the homogenized deformation is equal to the imposed macroscopic deformation (i.e., $\mathbf{E} = \mathbf{E}^*$). The computationally homogenized stress is obtained from the microscopic fields calculated by finite elements using the ANSYS[®] Mechanical, Release 18.0. The structured meshes of the RVEs are shown in Fig. 4. The quadratic hexahedral solid element with 20 nodes are used in numerical analysis. The sequence of meshes adopted are formed by 19992 elements, 85513 nodes and 256539 degrees of freedom. The expression to obtain the computationally homogenized stress (Σ) is given by:

$$\Sigma = \frac{1}{V} \sum_{i=1}^{N_{\text{elem}}} \sigma_i V_i, \quad (7)$$

where N_{elem} is the total number of finite elements; σ_i is the average stress in the element i computed at their integration points; V_i is the volume of the element i ; and V is the total volume of the RVE.

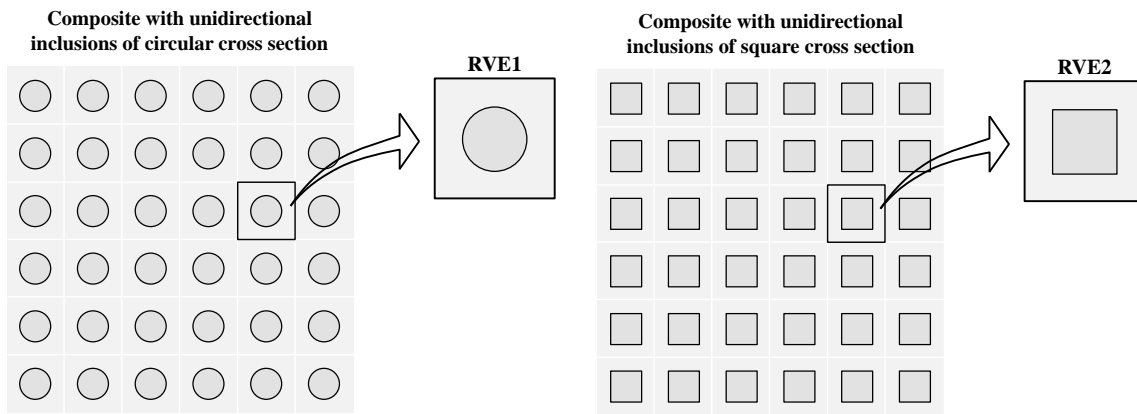


Figure 3. RVE morphologies of the study from composites with periodic distribution.

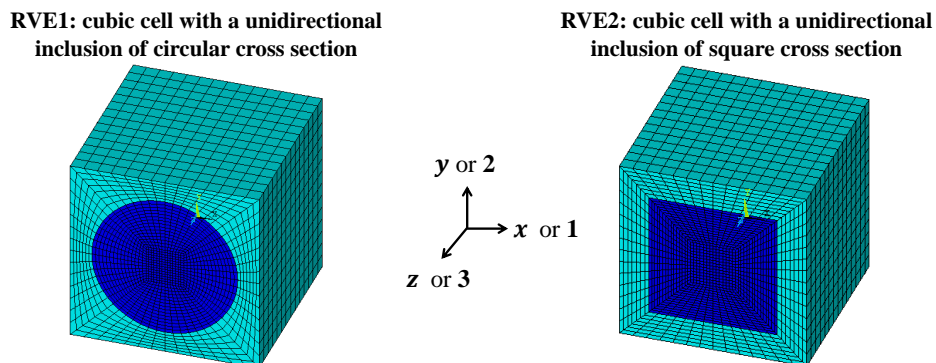


Figure 4. Meshes with 19992 elements, 85513 nodes and 256539 degrees of freedom.

The macroscopic constitutive behavior is assumed to be orthotropic and linearly elastic. The principal orientation of orthotropy is assumed to coincide with the cartesian reference directions. In this case, the constitutive law

in an equivalent matrix notation derived from the *Voigt notation*, in terms of \mathbb{C} and \mathbb{D} respectively, are given by:

$$\begin{pmatrix} \Sigma_{11} \\ \Sigma_{22} \\ \Sigma_{33} \\ \Sigma_{12} \\ \Sigma_{13} \\ \Sigma_{23} \end{pmatrix} = \begin{bmatrix} C_{11} & C_{12} & C_{13} & 0 & 0 & 0 \\ C_{12} & C_{22} & C_{23} & 0 & 0 & 0 \\ C_{13} & C_{23} & C_{33} & 0 & 0 & 0 \\ 0 & 0 & 0 & C_{44} & 0 & 0 \\ 0 & 0 & 0 & 0 & C_{55} & 0 \\ 0 & 0 & 0 & 0 & 0 & C_{66} \end{bmatrix} \begin{pmatrix} E_{11} \\ E_{22} \\ E_{33} \\ 2E_{12} \\ 2E_{13} \\ 2E_{23} \end{pmatrix} \quad (8a)$$

$$\begin{pmatrix} E_{11} \\ E_{22} \\ E_{33} \\ 2E_{12} \\ 2E_{13} \\ 2E_{23} \end{pmatrix} = \begin{bmatrix} \frac{1}{Y_1} & -\frac{\nu_{21}}{Y_2} & -\frac{\nu_{31}}{Y_3} & 0 & 0 & 0 \\ -\frac{\nu_{12}}{Y_1} & \frac{1}{Y_2} & -\frac{\nu_{32}}{Y_3} & 0 & 0 & 0 \\ -\frac{\nu_{13}}{Y_1} & -\frac{\nu_{23}}{Y_2} & \frac{1}{Y_3} & 0 & 0 & 0 \\ 0 & 0 & 0 & \frac{1}{G_{12}} & 0 & 0 \\ 0 & 0 & 0 & 0 & \frac{1}{G_{13}} & 0 \\ 0 & 0 & 0 & 0 & 0 & \frac{1}{G_{23}} \end{bmatrix} \begin{pmatrix} \Sigma_{11} \\ \Sigma_{22} \\ \Sigma_{33} \\ \Sigma_{12} \\ \Sigma_{13} \\ \Sigma_{23} \end{pmatrix} \quad (8b)$$

where $\nu_{12}Y_2 = \nu_{21}Y_1$; $\nu_{13}Y_3 = \nu_{31}Y_1$; $\nu_{23}Y_3 = \nu_{32}Y_2$.

The components C_{ij} of eq. (8a) were obtained from different loading situations considering \mathbf{E}^* . In the context of the studied kinematic boundary conditions, six numerical simulations were performed for each RVE: (1) $E_{11} = 1.0$; (2) $E_{22} = 1.0$; (3) $E_{33} = 1.0$; (4) $2E_{12} = 1.0$; (5) $2E_{13} = 1.0$; and (6) $2E_{23} = 1.0$. Therefore, the constitutive stiffness tensor (\mathbb{C}) was obtained by eq. (8a) considering the homogenized stress and strain tensors (Σ and E). The flexibility tensor (\mathbb{D}) was obtained by performing \mathbb{C}^{-1} . Finally, the elastic constants were determined by eq. (8b).

2.2 Results of effective elastic properties

The results for the effective elastic constants for the RVE1 considering the PBC are shown in the Table 1, including the comparison with the works of Xia et al. [7] and Sun and Vaidya [5]. The constants Y_2 and G_{31} are omitted for the sake of conciseness, since, due to the symmetry plane 2 – 3 of the RVEs, they are equal to Y_3 and G_{12} , respectively. The answers match very well with Xia et al. [7] results for all constants. The answers are also close to Sun and Vaidya [5] results for almost all constants. In this case, the most significant differences are those for the constants G_{23} and ν_{12} . Therefore, in general, the results of the homogenization procedure are close to the reference works.

Table 1. Effective elastic constants for the RVE1 considering the PBC.

Elastic parameter	Present work	Xia et al. [7]	Sun and Vaidya [5]	Differences in module	
	(1)	(2)	(3)	(1) to (2)	(1) to (3)
Y_1 (GPa)	144.00	143	144	0.70 %	0.00 %
Y_3 (GPa)	215.34	214	215	0.63 %	0.16 %
G_{12} (GPa)	45.82	45.7	45.9	0.26 %	0.18 %
G_{23} (GPa)	54.38	54.2	57.2	0.34 %	4.92 %
ν_{12}	0.2550	0.255	0.29	0.02 %	12.08 %
ν_{32}	0.1946	0.195	0.19	0.23 %	2.40 %

Table 2 shows the results of the effective elastic constants for each RVE morphology (RVE1 and RVE2) considering both studied boundary conditions (USBC and PBC). In addition to tables, visualization of microscopic

fields is also useful to understand macroscopic results. In this context, Figures 5 and 6 show the distributions of the microscopic shear stress (σ_{12}) for the RVEs submitted to the USBC and PBC, respectively, considering the loading situation with $2E_{12} = 1.0$.

The influence of the boundary condition in the results of the effective elastic constants are similar for both RVEs morphologies. For each of these configurations, there are strong differences between the results from USBC and PBC. The properties of G_{12} and G_{23} obtained with PBC are significantly lower compared to USBC, which indicates that the boundary condition plays an important role in the shear modulus. This can be explained by the difference in the distribution of microscopic stresses for each boundary condition (see Figs.5 and 6). The sensitivity of the response of the constant Y_1 is also observed, where the PBC indicates a response with a lower value. Moreover, there are differences in the ν_{12} and ν_{32} constants, where the responses with USBC are lower compared to PBC. In this case, the differences are more significant for ν_{12} parameter compared to ν_{32} parameter.

On the other hand, the influence of the inclusion morphology is small in the results of the effective elastic constants. The most significant difference occurs for the elastic constant ν_{12} . It is also valid to mention the smaller, but not negligible, divergences for the constants Y_1 and G_{12} .

Table 2. Comparison of the effective elastic constants between RVE1 and RVE2 for the USBC and the PBC.

Elastic parameter	RVE1		RVE2		Differences in module			
	USBC	PBC	USBC	PBC				
	(1)	(2)	(3)	(4)	(2) to (1)	(4) to (3)	(3) to (1)	(4) to (2)
Y_1 (GPa)	158.21	144.00	161.08	147.86	8.98 %	8.21 %	1.81 %	2.68 %
Y_3 (GPa)	216.09	215.34	216.08	215.37	0.35 %	0.33 %	0.00 %	0.01 %
G_{12} (GPa)	61.71	45.82	60.43	45.30	25.76 %	25.03 %	2.08 %	1.12 %
G_{23} (GPa)	72.18	54.38	72.39	54.85	24.65 %	24.23 %	0.30 %	0.85 %
ν_{12}	0.2288	0.2550	0.2145	0.2369	11.43 %	10.41 %	6.21 %	7.08 %
ν_{32}	0.1846	0.1946	0.1846	0.1941	5.37 %	5.13 %	0.00 %	0.23 %

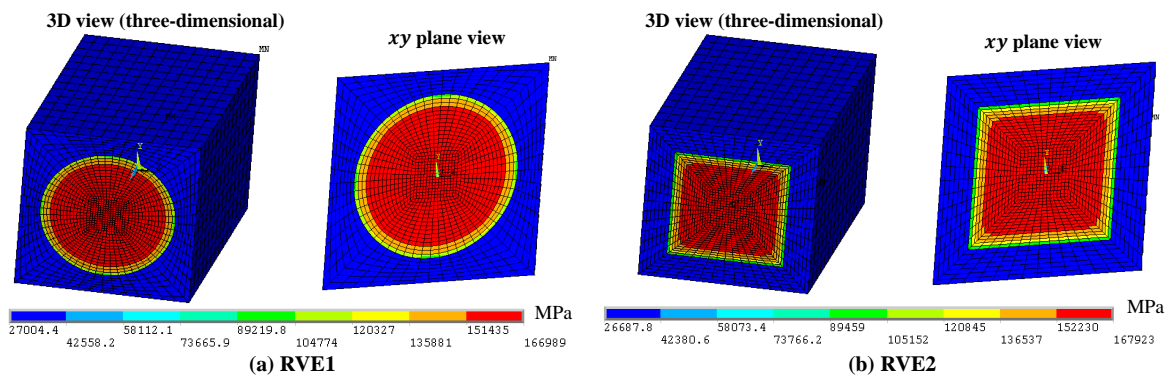


Figure 5. Microscopic shear stress distributions (σ_{12}) for USBC.

3 Conclusions

The present work carried out a study on the overall effective properties of composites using an approach based on computational homogenization. Two morphologies of RVE were assessed, considering both USBC and PBC. The restriction imposed on the external contour of the RVE clearly interferes in the distribution of its microscopic fields. Consequently, in general, the boundary condition has a significant influence in the results of the effective elastic constants, mainly for the constants associated with the shear modulus. In contrast, the change in the inclusion morphology has a clearer influence only on the Poisson's ratio for the plane associated with the fiber cross section. Therefore, in general, the inclusion morphologies considered in the present work do not play an important role in the results of the effective elastic constants. Moreover, the computational homogenization procedure implemented in the ANSYS[®] software is an interesting tool to study other problems with periodic materials.

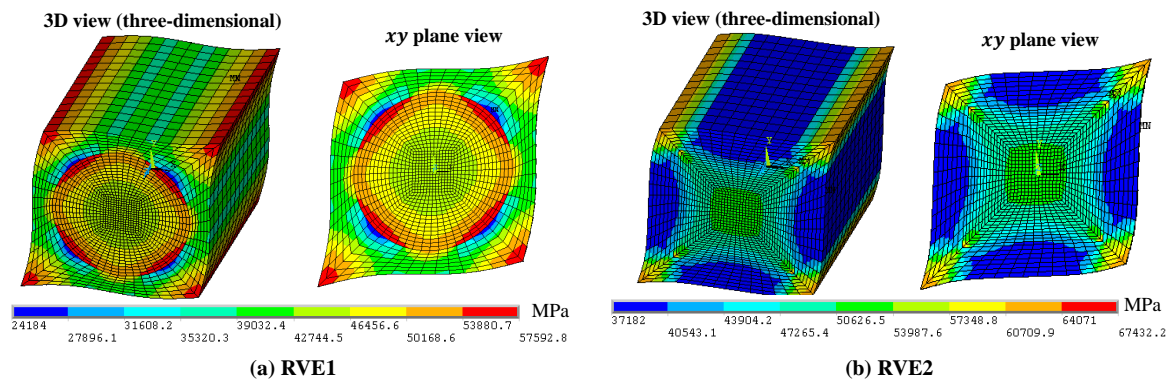


Figure 6. Microscopic shear stress distributions (σ_{12}) for PBC.

Acknowledgements. The authors would like to gratefully acknowledge Conselho Nacional de Desenvolvimento Científico e Tecnológico - Brasil (CNPq). This study was also financed by the Coordenação de Aperfeiçoamento de Pessoal de Nível Superior - Brasil (CAPES) - Finance Code 001.

Authorship statement. The authors hereby confirm that they are the sole liable persons responsible for the authorship of this work, and that all material that has been herein included as part of the present paper is either the property (and authorship) of the authors, or has the permission of the owners to be included here.

References

- [1] W. Voigt. Ueber die beziehung zwischen den beiden elasticitätsconstanten isotroper körper. *Annalen der Physik*, vol. 274, pp. 573–587, 1889.
- [2] A. Reuss. Berechnung der fließgrenze von mischkristallen auf grund der plastizitätsbedingung für einkristalle. *ZAMM - Journal of Applied Mathematics and Mechanics / Zeitschrift für Angewandte Mathematik und Mechanik*, vol. 9, pp. 49–58, 1929.
- [3] Z. Hashin and S. Shtrikman. A variational approach to the theory of the elastic behaviour of multiphase materials. *Journal of the Mechanics and Physics of Solids*, vol. 11, pp. 127–140, 1963.
- [4] R. Hill. Elastic properties of reinforced solids: Some theoretical principles. *Journal of the Mechanics and Physics of Solids*, vol. 11, pp. 357–372, 1963.
- [5] C. T. Sun and R. S. Vaidya. Prediction of composite properties from a representative volume element. *Composites Science and Technology*, vol. 56, pp. 171–179, 1996.
- [6] J. Michel, H. Moulinec, and P. Suquet. Effective properties of composite materials with periodic microstructure: a computational approach. *Computer Methods in Applied Mechanics and Engineering*, vol. 172, pp. 109–143, 1999.
- [7] Z. Xia, Y. Zhang, and F. Ellyin. A unified periodical boundary conditions for representative volume elements of composites and applications. *International Journal of Solids and Structures*, vol. 40, pp. 1907–1921, 2003.
- [8] S. Kari, H. Berger, R. Rodriguez-Ramos, and U. Gabbert. Computational evaluation of effective material properties of composites reinforced by randomly distributed spherical particles. *Composite Structures*, vol. 77, pp. 223–231, 2007.
- [9] R. d. Medeiros, M. E. Moreno, F. D. Marques, and V. Tita. Effective properties evaluation for smart composite materials. *Journal of the Brazilian Society of Mechanical Sciences and Engineering*, vol. 34, pp. 362–370, 2012.
- [10] S. L. Omairey, P. D. Dunning, and S. Sriramula. Development of an abaqus plugin tool for periodic rve homogenisation. *Engineering with Computers*, vol. 35, pp. 567–577, 2019.
- [11] J. F. W. Bishop and R. Hill. Xlvi. a theory of the plastic distortion of a polycrystalline aggregate under combined stresses. *Philosophical Magazine Series 5*, vol. 42, pp. 414–427, 1951.
- [12] J. Mandel. *Plasticité classique et viscoplasticité*. Springer-Verlag, Udine, Italy, 1971.
- [13] W. F. Santos. Computational modeling of the rupture of elasto-plastic media with initial voids. Master's degree in civil engineering (structural engineering), São Carlos School of Engineering, University of São Paulo, São Carlos, 2021.